ORIGINAL ARTICLE OPEN ACCESS

Simultaneous Activation of Beta-Oxidation and De Novo Lipogenesis in MASLD-HCC: A New Paradigm

Fatima Dahboul[1] | Jihan Sun[1,2] | Benjamin Buchard[1,3] | Natali Abeywickrama-Samarakoon[1] | Estelle Pujos-Guillot[4] | Stéphanie Durand[4] | Mélanie Petera[4] | Delphine Centeno[4] | Francesca Guerrieri[5,6] | Massimiliano Cocca[5,6] | Massimo Levrero[5,6,7] | Adrien Rossary[1] | Delphine Weil[2,8] | Vincent Di Martino[2,8] | Aicha Demidem[1] | Armando Abergel[3,9]

[1]Human Nutrition Unit 1019, INRAE, Clermont Auvergne University, Clermont-Ferrand, France | [2]EFS, INSERM, UMR RIGHT, Franche-Comté University, Besançon, France | [3]Department of Digestive and Hepatobiliary Medicine, CHU Clermont-Ferrand, Clermont-Ferrand, France | [4]Human Nutrition Unit 1019, Plate-Forme d'Exploration du Métabolisme, MetaboHUB—Clermont, INRAE, Clermont Auvergne University, Clermont-Ferrand, France | [5]INSERM U1052, CNRS UMR 5286, Cancer Research Center of Lyon (CRCL), Lyon, France | [6]Institute of Hepatology Lyon (IHL), Lyon, France | [7]Hepatology Department, Hospices Civils de Lyon and University of Lyon, Université Claude-Bernard Lyon 1 (UCBL1), Lyon, France | [8]Hepatology and Digestive Intensive Care Service, Jean Minjoz Hospital, Besançon, France | [9]Clermont Auvergne University, Clermont-Ferrand, France

Correspondence: Aicha Demidem (aicha.demidem@uca.fr; aicha.demidem@inrae.fr)

ABSTRACT

Background and Aims: Metabolic dysfunction-associated steatotic liver disease (MASLD) is the most common cause of hepatocellular carcinoma (HCC). In this study, we combine metabolomic and gene expression analysis to compare HCC tissues with non-tumoural tissues (NTT).

Methods: A non-targeted metabolomic strategy LC–MS was applied to 52 pairs of human MASLD-HCC and NTT separated into 2 groups according to fibrosis severity F0F1-F2 versus F3F4. The expression of genes related to de Novo lipogenesis (DNL) and fatty acid oxidation (FAO) has been analysed by quantitative RT-PCR and/or interrogation of RNA-seq datasets in 259 pairs of tissues (MASLD-HCC vs. VIRUS-HCC).

Results: Metabolomic analysis revealed that acylcarnitines were the main discriminating metabolites according to fibrosis severity when we compared MASLD-HCC-F0F1-F2 versus NTT and MASLD-HCC-F3F4 versus NTT. Based on these metabolomic data, the analysis of a panel of 15 selected genes related to DNL and FAO indicated that there is no difference between the 2 groups of MASLD-HCC. In contrast the same comparative gene analysis according to the aetiology of HCC: MASLD-HCC versus

---

VIRUS-HCC showed that both aetiologies shared the same upregulation of genes involved in DNL. However, five genes involved in FAO (HADHA, CRAT, CPT1, CPT2 and PPARA) are upregulated exclusively in MASLD-HCC. This result indicates that FAO and DNL pathways are simultaneously activated in MASLD-HCC in contrast to VIRUS-HCC.

Conclusions: These results suggest that, the involvement of adaptive metabolic pathways is different depending on the aetiology of HCC. Moreover, the dogma that simultaneous activation of FAO and DNL is incompatible in cancer would not apply to MASLD-HCC.

1 | Introduction

Hepatocellular carcinoma (HCC) is one of the most prevalent malignant neoplasms and the second most common cause of cancer-related mortality on a global scale [1]. HCC is a complication of several chronic liver diseases, including hepatitis B and C virus infection and metabolic dysfunction-associated steatotic liver disease (MASLD) [2].

The global prevalence of MASLD has increased markedly over the past few decades, in parallel with the epidemics of obesity and type 2 diabetes [3]. This has led to an increase in the prevalence of HCC [4]. Twenty percent of MASLD-associated HCC (MASLD-HCC) cases lack evidence of cirrhosis [5, 6]. Despite the established role of insulin resistance and PNPLA3 polymorphism [7] and the increasing evidence suggesting that epigenetic modifications play a significant role in the occurrence and progression of MASLD to HCC [8], the precise mechanisms underlying the disease in only a subset of these patients remain unclear. This lack of knowledge impedes the precise identification of patients who are at risk and thus require surveillance.

As a consequence, HCC in MASLD, particularly in the absence of associated cirrhosis, is more likely to be detected at a more advanced tumour stage [5]. Therefore, although the annual incidence of HCC in non-cirrhotic patients with MASLD remains much lower than in cirrhotic patients and does not justify screening all patients with MASLD for HCC [9, 10], a 1.2-fold higher mortality rate has been observed in patients with HCC developed in MASLD compared to patients with HCC of other aetiologies [11].

The ultimate objective of our research is to identify a metabolomic and molecular signature of patients with HCC associated with MASLD without cirrhosis, which could potentially be utilised in the future for non-invasive diagnostic or screening purposes. In our previous study, two metabolomic phenotypes of human MASLD-HCC were identified according to fibrosis severity using ^{1}H-nuclear magnetic resonance spectroscopy (NMR) analysis [12, 13]. The findings have revealed the existence of diverse signalling pathways and distinct mechanisms of carcinogenesis, which vary depending on the level of fibrosis.

The objectives of the present study were: (1) to gain a deeper understanding of the processes influencing the expression of different metabolites in tumoural tissue (TT) as compared with non-tumoural tissue (NTT) in patients with MASLD-HCC. To this end, we conducted comprehensive metabolomic and gene expression analysis on liver tissues and compared non-tumour tissue (NTT) to HCC tissue (TT) in two MASLD-HCC groups, including a comparison between F0F1-F2 and F3F4 MASLD

patients, to study the effect of liver fibrosis; (2) to study the effect of aetiology, the hepatic gene expression profiles of MASLD-HCC patients were compared with those of VIRUS-HCC patients to better identify a molecular signature specific to MASLD-HCC.

2 | Patients and Methods

2.1 | Patients and Collection of Specimens MASLD-HCC

Liver tissue samples were obtained from surgical specimens and collected from the French Liver Biobank (CRB Foie). For each patient, tumour tissue (TT) and adjacent non-tumour tissue (NTT) were provided. The 98 patients were selected according to the following criteria: (1) dysmetabolic liver disease without other associated causes, (2) stage of fibrosis defined with the METAVIR score by histological analysis, (3) balanced distribution of tumour differentiation stage (well or moderately differentiated). Clinical, biological and histological characteristics of the two groups are shown in Table S1, panel A. The study was approved by the Sud-Est VI Clermont-Ferrand Ethics Committee (agreement number AU887, 04/03/2011).

2.2 | Patients and Datasets of VIRUS-HCC

The datasets pertaining to hepatitis virus-related HCCs comprise five distinct cohorts for a total of 161 patients with paired liver TT and NTT samples 59 patients with HBV-related HCC and 102 patients with HCV-related HCC. (see Table S1 panel B).

2.3 | Healthy Controls and MASLD Liver Tissues From Patients

Control liver tissues were obtained from the French Liver Biobank ($n = 13$) (see Table S1 panel C). The normal liver tissues were obtained from patients undergoing focal nodular hyperplasia (FNH) hepatectomy. FNH is defined as the development of a benign hepatocyte tumour comprising hepatocytes forming regeneration nodules in the presence of a fibrous scar, traversed by dystrophic arteries [14]. The hepatic parenchyma surrounding the benign tumour is regarded as healthy tissue, devoid of hepatocyte abnormalities and is utilised as a control tissue. The exclusion criteria were as follows: subjects with a BMI less than $18.5 \, \text{kg/m}^2$ or greater than $25 \, \text{kg/m}^2$, as well as those with type 2 diabetes, chronic liver disease and/or metastases and excessive alcohol consumption were excluded from the study. Liver tissue from our cohort of MASLD patients ($n = 17$) was obtained from Professor Levrero

Summary

- The Acyl-carnitines profile exhibits variability in MASLD-HCC contingent upon the severity of fibrosis.
- Both fatty acid oxidation (FAO) and de Novo lipogenesis (DNL) are activated in MASLD-HCC.
- Different adaptive metabolic pathways are involved depending on the aetiology of HCC, with MASLD-HCC and VIRUS-HCC displaying distinct profiles.
- MASLD-HCC differs from VIRUS-HCC in the expression of five genes implicated in the FAO pathways. CPT1, CPT2, HADHA, CRAT and PPARA were found to be upregulated in MASLD-HCC whereas the expression of these genes was observed to be downregulated in VIRUS-HCC.
- The simultaneous activation of FAO and DNL may be regarded as a distinctive feature of MASLD-HCC irrespective of the degree of fibrosis.

and Dr. M.L. Plissonnier of the Cancer Research Center of Lyon, France (see Table S1 panel D).

2.4 | Histology

The tissues were fixed in 10% formalin and subsequently embedded in paraffin for light microscopy. Paraffin sections with a thickness of $5\,\mu m$ were subjected to staining with the haematoxylin and eosin method. The specific type and differentiation of the HCC were determined in accordance with the WHO classification. The NTT was characterised by the presence or absence of lesions of chronic hepatitis, fibrosis, steatosis and steatohepatitis as well as the METAVIR Score.

2.5 | Human Cell Cultures (HepG2)

To investigate the relationship between fatty acid oxidation (FAO) and DNL, we performed gene expression analysis on HepG2 cell cultures treated with the CPT inhibitor, aminocarnitine. The mRNA expression levels of key metabolic genes were measured, including citrate synthase (CS), ATP citrate lyase (ACLY), acetyl-CoA carboxylases (ACC1 and ACC2), fatty acid synthase (FASN), carnitine palmitoyltransferases (CPT1 and CPT2), hydroxyacyl-CoA dehydrogenase (HADHA), and peroxisome proliferator-activated receptor alpha (PPARA).

Low passage HepG2 cell line was obtained from Dr. ML Plissonnier at the Cancer Research Center of Lyon, France. For maintenance, HepG2 cells were cultured in Dullbecco's Modified Eagle's Medium (DMEM, Sigma–Aldrich) containing 10% foetal bovine serum (ThermoFisher Scientific), 1% L-Glutamine (Sigma–Aldrich), and 1% penicillin–streptomycin (ThermoFisher Scientific). The cells were incubated in an environment with 85% humidity, maintained at 37°C and with 5% CO_2 supplementation.

2.6 | Metabolomic Analysis

The Data S1 provides a detailed account of the procedure for the extraction of metabolites, the experimental settings for liquid chromatography coupled to high-resolution mass spectrometry, the data processing tools and the metabolite annotation.

2.7 | Gene Expression Analysis by qRT-PCR

Gene expression analysis by qRT-PCR was performed in TT and NTT from MASLD-HCC patients, disease control patients and healthy livers, as well as in HepG2 cells. A total of 226 samples were extracted, comprising 98 pairs of MASLD-HCC (Cohort 1, see panel A in Table S1 for details), 13 healthy samples (see panel C in Table S1 for details) and 17 MASLD liver tissues (see panel D in Table S1 for details). mRNA expression levels of the following metabolic genes including CS, ACLY, ACC1, ACC2, FASN, stearoyl-CoA desaturase 1 (SCD1), sterol regulatory element-binding protein 1 (SREBP-1), CPT1, CPT2, acyl CoA dehydrogenase short chain (ACADS), acyl CoA dehydrogenase very long chain (ACADVL), HADHA, carnitine acetyltransferase (CRAT), carnitine octanoyl-transferase (CROT) and PPARA were measured by RT-PCR.

Total RNA was extracted from frozen liver tissues and HepG2 cells using a commercially available kit (Qiagen GmbH, Germany) in accordance with the manufacturer's instructions. For cell culture, total RNA was extracted using TRIzol reagent (Invitrogen) in accordance with the manufacturer's instructions. The purity and the quality of the RNA were evaluated using a NanoDrop spectrophotometer (model ND-1000, Thermo Fisher Scientific). The synthesis of complementary DNA (cDNA) was conducted using the SuperScript VILO cDNA Synthesis Kit (Invitrogen). The sequence of primers utilised for qRT-PCR can be found in Table S2. All reactions were conducted in triplicate using the Power Up SYBR Green Master Mix (Thermo Fisher Scientific). The relative gene expression levels in liver tissues and HepG2 cells were calculated after normalisation to 18S rRNA and GAPDH, respectively, using the ΔΔCT method (Bio-Rad Laboratories). A stability analysis of housekeeping genes, including β-actin, GAPDH, HPRT and 18S rRNA, was conducted using NormFinder. The results demonstrated that 18S rRNA and GAPDH exhibited the highest stability in liver tissues and HepG2 cells, respectively.

2.8 | RNA-Seq, Data Download and Normalisation Method

RNA-seq datasets from 5 cohorts of VIRUS-HCC were interrogated for the expression of the above-mentioned set of metabolic genes.

For Cohort 2 (10 pairs of HBV-related HCCs from the Lyon HCC cohort, see panel B in Table S1 for details) mRNA libraries were prepared from both TT and NTT frozen tissues using the TruSeq Stranded RNA HT (w/Ribo-Zero) kit with the objective of increasing the depth of sequencing. Each library

was subjected to paired-end sequencing, yielding an average of 30–40 million reads per sample. This was conducted using 75×2 cycles on a NextSeq 500 Illumina platform. The data were aligned to the GRCh38 reference genome build using the STAR aligner [https://doi.org/10.1093/bioinformatics/bts635]. The raw gene expression counts were generated using the STAR aligner.

The International Cancer Genome Consortium (ICGC) Japanese liver cancer (ICGC-LIRI-JP) data were obtained using the R package ICGC tools R (https://github.com/yikeshu0611/ICGCtoolsR/), as previously utilised [15]. Forty-three TT and NTT paired samples from HBV-related HCCs (Cohort 3) and 98 TT and NTT paired samples from HCV-related HCCs (Cohort 5) (see panel B in Table S1 for details).

The mRNA expression data from the Cancer Genome Atlas Liver Hepatocellular Carcinoma (TCGA-LIHC) project [https://doi.org/10.1016/j.cell.2017.05.046] were downloaded using the R package TCGA biolinks (http://doi.org/10.1093/nar/gkv1507). A total of 10 paired TT and NTT samples were selected for analysis, comprising six HBV-HCCs (Cohort 4) and four HCV-HCCs (Cohort 6) (see panel B in Table S1 for details).

The raw RNA-seq counts were imported into a DESeq2 dataset object for normalisation using the variant stabilising transformation (VST) for the purposes of data visualisation and differential expression analysis.

2.9 | Measurement of CPT1 and CPT2 Activity

The activities of the mitochondrial CPT1 and CPT2 were quantified in accordance with a methodology previously described [16]. In brief, $50\,\mu g$ of crude mitochondrial suspension were incubated in assay medium (20 mM HEPES, 1 mM EGTA, 220 mM sucrose, 40 mM KCl, 0.1 mM DTNB, 1.3 mg/mL bovine serum albumin and $40\,\mu M$ palmitoyl-CoA) in a 96-well microplate, to which 1 mM carnitine was added to measure total CPT activity. The spectrophotometer was used to monitor the absorbance of the solution at 405 nm for a period of 15 min. CPT2 activity was quantified using the identical reaction mixture employed for total CPT activity, with the inclusion of $10\,\mu M$ malonyl-CoA, a known inhibitor of CPT1. CPT1 activity was calculated by subtracting CPT2 activity from the total CPT activity. The results were normalised to mitochondrial protein content.

2.10 | MTT Assay of Amino-Carnitine Treatment

A total of 10^3 HepG2 cells in $200\,\mu L$ of medium were seeded into 96-well plates and allowed to grow for 24 h. Thereafter, the cells were treated with amino-carnitine (Santa Cruz) at concentrations of 0, 0.25, 0.5, 0.75, and 1 mM for 24, 48 and 72 h. Twenty microliters of MTT (3-(4,5-dimethylthiazol-2-yl)-2,5-diphenylte trazolium bromide) were added to each well and incubated for 4 h at 37°C. The absorbance at 570 nm was quantified using a plate reader (Tecan Spark, Männedorf, Switzerland). The cell viability, which is proportional to the absorbance, was reported as a relative decrease in comparison to the absorbance resulting from the control, which was considered to be 100% viable cells.

The results presented here are the mean values and Standard error of the mean (SEM) from at least three independent experiments, each performed in triplicate.

2.11 | Statistical Analysis

All data are reported as the mean $\pm$ SEM. The statistical significance of differences between experimental groups was evaluated using the Wilcoxon rank-order test and the Kruskal–Wallis test. A p-value of less than 0.05 was considered statistically significant. All Statistical analyses were performed using the GraphPad Prism 8.1.2 software.

3 | Results

3.1 | Metabolomic Analyses in MASLD-HCC

3.1.1 | Comparison Between Tumour and Non-Tumour Tissues Regardless of Liver Fibrosis

An untargeted metabolomic LC–MS analysis was conducted on 52 paired samples of MASLD-HCC (TT vs. NTT), resulting in the extraction of a total of 1290 metabolites and related features. Following univariate statistical analysis, 65 and 152 metabolites related features were identified as significantly different between NTT and TT ($p < 0.05$, after Benjamini-Hochberg correction) in the MASLD-HCC-F0F1-F2 and MASLD-HCC-F3F4 groups, respectively (see Table S3). It is noteworthy that only 12 compounds are shared by both the MASLD-HCC-F0F1-F2 and MASLD-HCC-F3F4 groups. Of the selected metabolites, 13 and 28, respectively, were successfully annotated for MASLD-HCC-F0F1-F2 (Table 1) and MASLD-HCC-F3F4 (Table 2). The majority of the identified metabolites were classified as belonging to the acylcarnitine (AC) family, the metabolism of the nucleotides, the glycolysis pathway, the urea cycle, amino acids and one-carbon metabolism.

3.1.2 | Comparison Between Tumour and Non-Tumour Tissues in F0F1-F2 Patients

An untargeted LC–MS analysis was conducted to identify metabolites in tumoral tissue (TT) and the paired NTT. MASLD-HCC-F0F1-F2 was distinguished by a notable elevation in 12 metabolites and a sole reduction in one metabolite (Table 1). MASLD-HCC-F0F1-F2 was distinguished by an accumulation of long-chain acylcarnitines (LCAC; 16–20 carbon atoms), encompassing both saturated and mono- and polyunsaturated acylcarnitines, in comparison with NTT-F0F1-F2.

3.1.3 | Comparison Between Tumour and Non-Tumour Tissues in F3F4 Patients

A comparison of the MASLD-HCC-F3F4 and NTT-F3F4 samples revealed the presence of 28 distinct metabolites in the former. MASLD-HCC-F3F4 exhibited a notable reduction in 17 metabolites and an accumulation of 11 metabolites (Table 2). In contrast to MASLD-HCC-F0F1-F2, MASLD-HCC-F3F4 was

TABLE 1 | Differentially changed metabolites in MASLD-HCC-F0F1-F2.

Types and names of metabolites	*m/z* (Da)	Retention time(min)	Log$_2$ fold change (TT vs. NTT)	*p*
Acylcarnitine metabolites				
Palmitoyl-carnitine (C16/LCAC)	400.3423	14.62	1.6	0.02
Hydroxyhexadecanoylcarnitine (C16/LCAC)	416.3372	13.58	1.6	0.02
Stearoyl-carnitine (C18/LCAC)	428.3736	15.46	1.6	0.03
Hydroxyoctadecenoylcarnitine (C18/LCAC)	262.1467	6.24	2.0	0.004
12-Hydroxy-12-octadecanoylcarnitine (C18/LCAC)	444.3686	14.52	1.5	0.02
Octadecenoylcarnitine (C18/LCAC)	426.358	14.83	1.6	0.01
Arachidoylcarnitine (C20/LCAC)	456.405	16.18	1.6	0.05
(11Z,14Z)-Eicosadienoylcarnitine (C20/LCAC)	452.3737	15.04	2.3	0.02
(11Z)-Eicosenoylcarnitine (C20/LCAC)	454.3893	15.58	1.9	0.01
Other metabolites				
Hypoxanthine	137.0458	1.45	0.7	0.04
Tryptophan	205.0971	7.44	0.5	0.05
Theobromine	184.0733	1.18	0.5	0.05
N1-Methyl-2-pyridone-5-carboxylic acid	153.0657	1.16	[a]−1.2	0.02

[a]Indicates TT decreased.

distinguished by the expression of three categories of AC, contingent on their chain length. This included an accumulation of both long-chain ACs (LCAC; 14–20 carbon atoms) and medium-chain ACs (MCAC; 8–12 carbon atoms). Conversely, short-chain ACs (SCAC; 2–6 carbon atoms), derived from isoleucine and leucine, were diminished in comparison with NTT-F3F4. Consequently, our LC–MS metabolomic analysis demonstrated discrepancies in the AC profile between the two of MASLD-HCC groups as illustrated in Figure 1.

3.2 | Gene Expression Analysis in MASLD-HCC

3.2.1 | Comparison of Gene Related to Metabolites Expression in Tumour and Non-Tumour Tissues

To gain deeper insight into the metabolic fingerprint observed in the two groups of MASLD-HCC, we conducted an analysis of the gene expression levels of 15 genes encoding enzymes involved in the metabolism of the identified metabolites. Quantitative RT-PCR was conducted on paired TT and adjacent NTT. Given the accumulation of AC in tumour tissues of MASLD-HCC, we conducted further investigations into the expression of hepatic enzymes that are primarily involved in the DNL and FAO pathways.

3.2.2 | De Novo Lipogenesis Genes in Patients With MASLD-HCC

The expression of seven genes, CS, ACLY, ACC1, ACC2, FASN, SCD1 and SREBP-1, encoding the primary enzymes involved in

de Novo lipogenesis (DNL) was analysed. The results presented in Figure 2A,B shown that the expression of mRNA transcripts encoding CS (catalyses the citrate synthesis from oxaloacetate), ACLY (cleaves citrate into acetyl-CoA and oxaloacetate), ACC1 (responsible for carboxylation of acetyl-CoA to produce malonyl-CoA), FASN (synthesises palmitic acid (C16:0)), and SCD1 (catalyses the rate-limiting step in the formation of mono-unsaturated fatty acids (MUFAs)) was significantly increased in both MASLD-HCC groups (F0F1-F2 and F3F4) compared with their adjacent NTT tissues, irrespective of the severity of fibrosis.

However, the mRNA expression of ACC2 and SREBP-1 (a master regulator of FA synthesis) remained unaltered in both MASLD-HCC (F0F1-F2 and F3F4), regardless the degree of fibrosis. The data suggest a significant energy demand in the tissues of MASLD-HCC, along with an excess of free FAs (FFA). These findings are reinforced when MASLD-HCC were compared with healthy liver tissues. Specially, the mRNA expression of CS, ACLY, ACC1, and FASN genes was significantly up-regulated in the two groups of MASLD-HCC compared with HL tissues, with the exception of ACC2, which remained unchanged (see Figure S1A).

3.2.3 | Fatty Acid Oxidation Genes in Patients With MASLD-HCC

A gene set analysis pertaining to FAO including CPT1, CPT2, ACADS, ACADVL, HADHA, CRAT, CROT and PPARA was performed. The mRNA expression levels of CPT1 and CPT2 (a rate-limiting enzyme for b-oxidation of long-chain fatty acids in mitochondria), HADHA (catalyses the last three steps of

TABLE 2 | Differentially changed metabolites in MASLD-HCC-F3F4.

Types and names of metabolites	*m/z* (Da)	Retention time (min)	Log$_2$ Fold Change (TT vs. NTT)	*p*
Acylcarnitine metabolites				
Butyryl carnitine (C4/SCAC)	232.1543	6.97	0.5	0.02
Tiglylcarnitine (C4/SCAC)	244.1543	7.68	[a]−1.2	0.02
Hydroxyisovaleroyl carnitine (C5/SCAC)	262.1647	6.24	[a]−1.3	0.02
Hexanoylcarnitine (C6/SCAC)	260.1855	8.79	[a]−1.6	0.01
Pimelycarnitine (C7/SCAC)	304.1754	7.43	[a]−1.3	0.03
Dodecenoylcarnitine (C12/MCAC)	342.2641	12.19	0.9	0.02
2-Hydroxydodecanoylcarnitine / 3-Hydroxydodecanoylcarnitine (C12/MCAC)	360.2747	11.59	0.6	0.03
Tetradecenoylcarnitine (C14/LCAC)	370.2954	13.18	1.0	0.03
3-Hydroxytetradecanoylcarnitine / 2-Hydroxymyristoylcarnitine (C14/LCAC)	388.306	12.61	0.6	0.03
Palmitoyl-carnitine (C16/LCAC)	400.3423	14.62	0.8	0.02
Hydroxypalmitoylcarnitine (C16/LCAC)	416.3372	13.58	0.6	0.03
Hexadecenoylcarnitine (C16/LCAC)	398.3267	14.02	1.1	0.01
12-Hydroxy-12-octadecanoylcarnitine (C18/LCAC)	444.3686	14.52	0.7	0.03
3-Hydroxy-11Z-octadecenoylcarnitine (C18/LCAC)	422.3529	13.90	1.1	0.01
Other metabolites				
Sarcosine/Alanine	90.0548	1.18	[a]−0.3	0.02
Glucose	203.3527	1.20	[a]−1.1	0.01
Betaine	118.0861	0.90	[a]−0.6	0.01
Creatine	132.0768	1.18	[a]−1.0	0.02
Nicotinamide	12.0552	1.16	[a]−1.0	0.01
Xanthosine	153.0406	6.29	[a]−0.7	0.01
Dihydrothymine	129.0659	0.93	[a]−1.4	0.03
N-Methyl-6-oxo-1,6-dihydropyridine-3-carboxylic acid	310.1134	0.93	[a]−1.0	0.01
Uric acid	169.0356	1.15	[a]−0.7	0.02
Tryptophan 2-C-mannoside	367.1499	6.21	[a]−0.9	0.01
Succinic anhydride	101.0234	2.11	[a]−0.6	0.03
N-Acetylneuraminic acid	310.1134	0.93	[a]−0.6	0.01
Histamine	112.0873	0.79	[a]−2.6	0.01
Urea/N-Nitrosomethylamine	61.0393	0.92	0.2	0.03

[a]Indicates TT decreased.

mitochondrial b-oxidation of long-chain fatty acids), CROT and CRAT (catalyses the interconversion of acetyl-CoA and acetyl carnitine) and PPARA (stimulates the import of acyl-CoA into the mitochondria by upregulating the expression of carnitine cycle members) were significantly increased in the two groups of MASLD-HCC (F0F1-F2, F3F4), irrespective of the level of fibrosis, when compared with their own NTT (Figure 2C,D). Furthermore, the expression of RNA encoding for ACADVL and ACADS (involved in the transport of very long-chain FA and short-chain FA, respectively) remained unchanged regardless of the severity of fibrosis.

Similarly, the aforementioned observations were corroborated when MASLD-HCC were compared with healthy liver tissues. The mRNA expression levels of CPT1, CPT2, HADHA, CRAT, CROT and PPARA were up-regulated in both groups
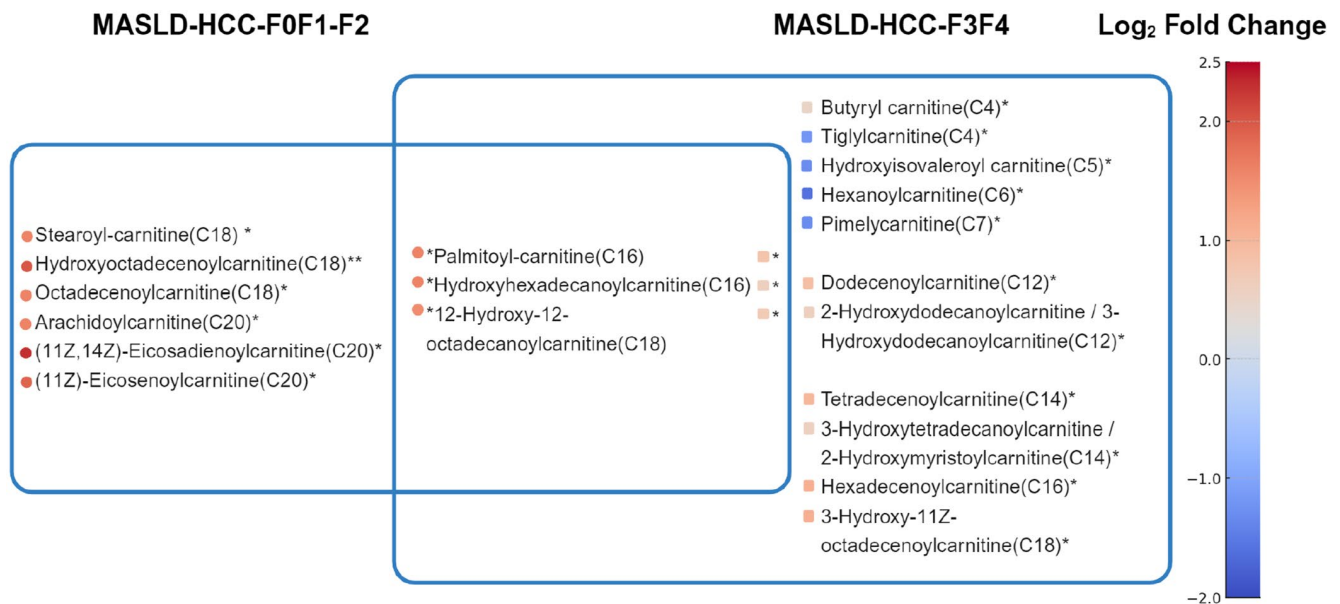
FIGURE 1 | Venn diagram displaying the distinct and overlapping carnitine metabolites identified in MASLD-HCC-F0F1-F2 and MASLD-HCC-F3F4. The colour-coding system used for the metabolites is based on their Log_2 Fold Change ratio between tumour and non-tumour tissues. The circles represent metabolites that are associated with MASLD-HCC-F0F1-F2, while the squares indicate metabolites that are associated with MASLD-HCC-F3F4. NS: No statistically significant differences were observed, *$p < 0.05$, **$p < 0.01$, ***$p < 0.001$ (Wilcoxon test).

HCC-F0F1-F2 and HCC-F3F4 versus healthy (see Figure S1B). Moreover, the expression of ACADS was exclusively up-regulated in HCC-F3F4. This result is consistent with our findings from the LC–MS metabolomics analysis. The overexpression of ACADS may be related to microbiota derived butyryl-carnitine, as reported in the identified metabolites by LC–MS (Table 2).

However, our study demonstrated that the expression of CPT2 in MASLD-HCC was markedly increased in both HCC and MASLD-adjacent tissues, as illustrated in Figure S2.

The data collectively demonstrate that the FAO is markedly-activated in both MASLD-HCC groups, irrespective of the degree of fibrosis. It is noteworthy that FAO is upregulated concurrently with DNL, which occurs predominantly through ACC1 rather than ACC2.

3.3 | Gene Expression Analysis in VIRUS-HCC

Our gene expression results in MASLD-HCC appear to be inconsistent with those previously reported for HCC developed in the context of HBV and/or HCV. To gain further insight into this discrepancy, we conducted a comparative analysis of the observed data according to the aetiology of HCC (i.e., MASLD-HCC vs. VIRUS-HCC). We examined the expression of the same panel of gene in the context of VIRUS-HCC, including those associated with HBV and HCV infections.

3.3.1 | Comparison of De Novo Lipogenesis in Patients With VIRUS-HCC and MASLD-HCC

The mRNA expression levels of genes encoding for the enzymes involved in the initial stages of DNL, including CS, ACLY, ACC1,

FASN and SCD1, was significantly increased in VIRUS-HCC groups (HBV and HCV) compared to their adjacent NTT tissues. However, the expression level of genes encoding for ACC2 and SREBP-1 was found to be down-regulated in the case of VIRUS-HCC (Figure 3A).

These results indicate that the expression of DNL-related genes was significantly increased in all HCC groups, irrespective of the underlying aetiology, which included MASLD-HCC and VIRUS-related HCC. However, the expression of ACC2 and SREBP-1 varied; it remained unchanged in the MASLD-HCC group and decreased in the VIRUS-HCC groups.

3.3.2 | Comparison of Fatty Acid Oxidation in Patients With VIRUS-HCC and MASLD-HCC

As illustrated in Figure 3B, the mRNA expression of CPT1, CPT2, ACADS, ACADVL, HADHA, CRAT and PPARA was significantly decreased in VIRUS-HCC groups (HBV and HCV) compared to their adjacent NTT tissues. However, the expression level of gene encoding for CROT was found to be unchanged in HBV and HCV induced VIRUS-HCC groups. These results indicate that the expression of FAO-related genes is differentially expressed according to the aetiology; with the expression of CPT1, CPT2, HADHA, CRAT, CROT and PPAR being increased exclusively in MASLD-HCC, while decreased in HBV and HCV induced VIRUS-HCC groups.

3.4 | Gene Expression Analyses in HepG2 Cells

A cytotoxicity test was performed on HepG2 cells using the MTT assay to evaluate the effects of amino-carnitine treatment at varying concentrations (0, 0.25, 0.5, 0.75, and 1 mM) and treatment
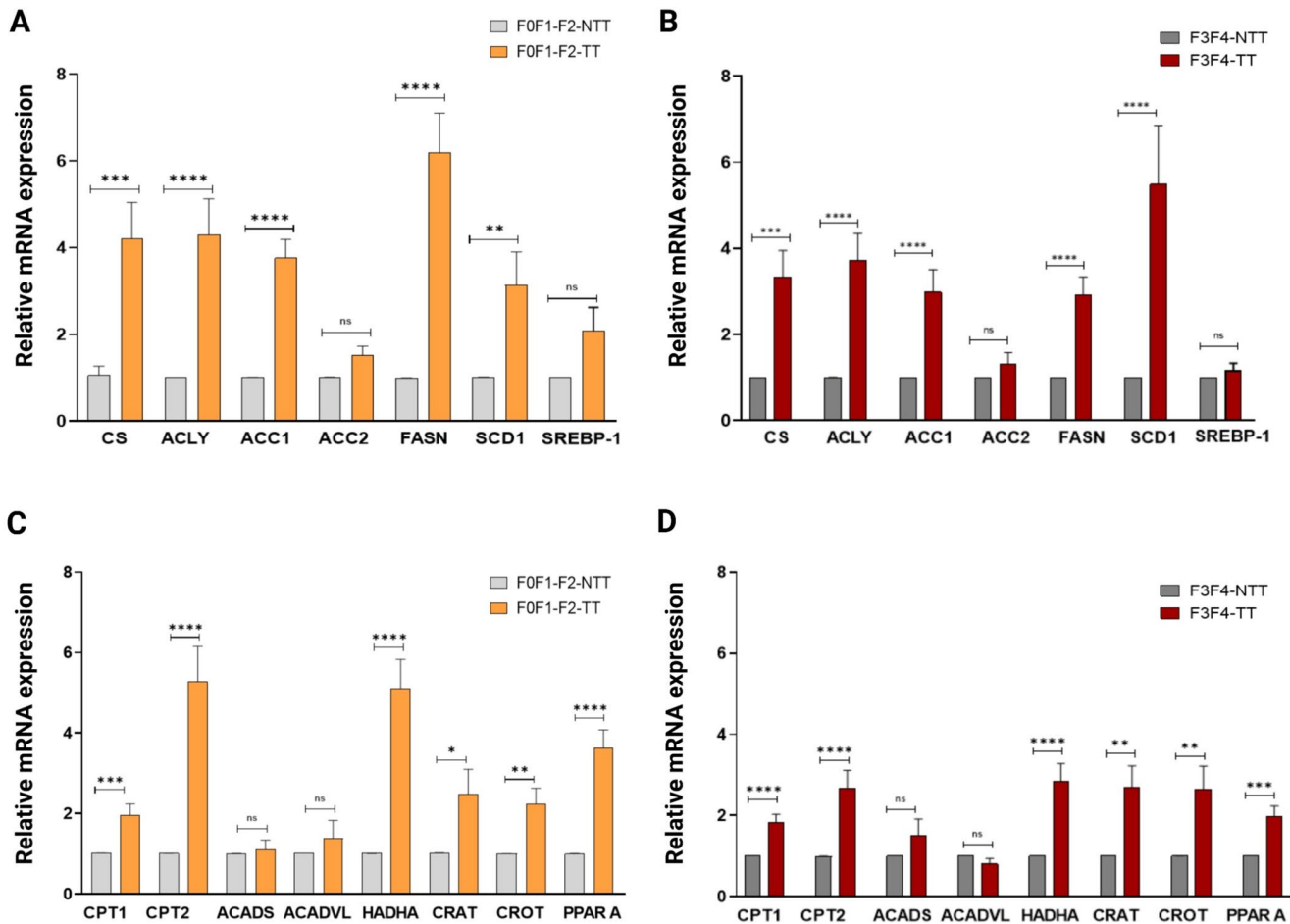
FIGURE 2 | Metabolic genes expression of MASLD-HCC versus MASLD-NTT by Quantitative real-time PCR (qRT-PCR). (A, B) The expression profile of six genes involved in the de Novo lipogenesis (DNL) pathway was compared between MASLD-HCC-F0F1-F2 and MASLD-HCC-F3F4, and between NTT-F0F1-F2 and NTT-F3F4, respectively. (C, D) The expression profile of eight genes related to the fatty acid oxidation (FAO) pathway was examined between MASLD-HCC-F0F1-F2 and MASLD-HCC-F3F4, with NTT-F0F1-F2 and NTT-F3F4 serving as the control groups. The data are expressed as the mean ± standard error of the mean (SEM). NS: No statistically significant differences were observed, *$p < 0.05$, **$p < 0.01$, ***$p < 0.001$ (Wilcoxon test).

durations (24, 48, and 72h). The results indicated that, at all concentrations tested, the cell survival rate remained close to 90% after 24, 48, and 72h of treatment (Figure 4A). These findings suggest that amino-carnitine did not significantly inhibit the proliferation of HepG2 cells under the conditions tested, indicating a lack of cytotoxicity at the concentrations and time points evaluated.

Moreover, to ascertain whether amino-carnitine induces or impedes the enzymatic activity and/or protein levels of the CPT system, we conducted enzymatic activity assays and protein level determinations in HepG2 cells. As illustrated in Figure 4B, the relative specific activity of CPT1 and CPT2 was significantly decreased in presence of amino-carnitine. Notably this inhibition is more pronounced in CPT2 compared to CPT1 as evidenced by the reduction in CPT2 activity observed in the cell line. These results corroborate those of previous studies [16, 17]. Furthermore, CPT2 inhibition results in a reduction in protein levels in HepG2 cells (see Figure S3).

The analysis of the expression of 9 selected genes related to the FAO (CPT1, CPT2, HADHA, and PPARA) and FAO (CS, ACLY,

ACC1, ACC2, and FASN) indicates that exposure of HepG2 cells to amino-carnitine induces a downregulation of genes involved in both the FAO and DNL pathways in a concentration-dependent manner (Figure 4C,D).

4 | Discussion

In the present study, we demonstrated, that the two groups of MASLD-HCC differed in the composition of AC according to the fibrosis score, MASLD-HCC-F0F1-F2 versus MASLD-HCC-F3F4. Secondly, we showed that the profile of metabolic-related gene expression, especially those involved in FAO, differed depending on the aetiology of HCC: MASLD-HCC versus VIRUS-HCC.

As previously reported, two metabolic phenotypes of MASLD-HCC have been identified according to the severity of fibrosis [12]. Nevertheless, the metabolic profile of MASLD-HCC and the expression of genes involved in metabolism remain to be fully elucidated.
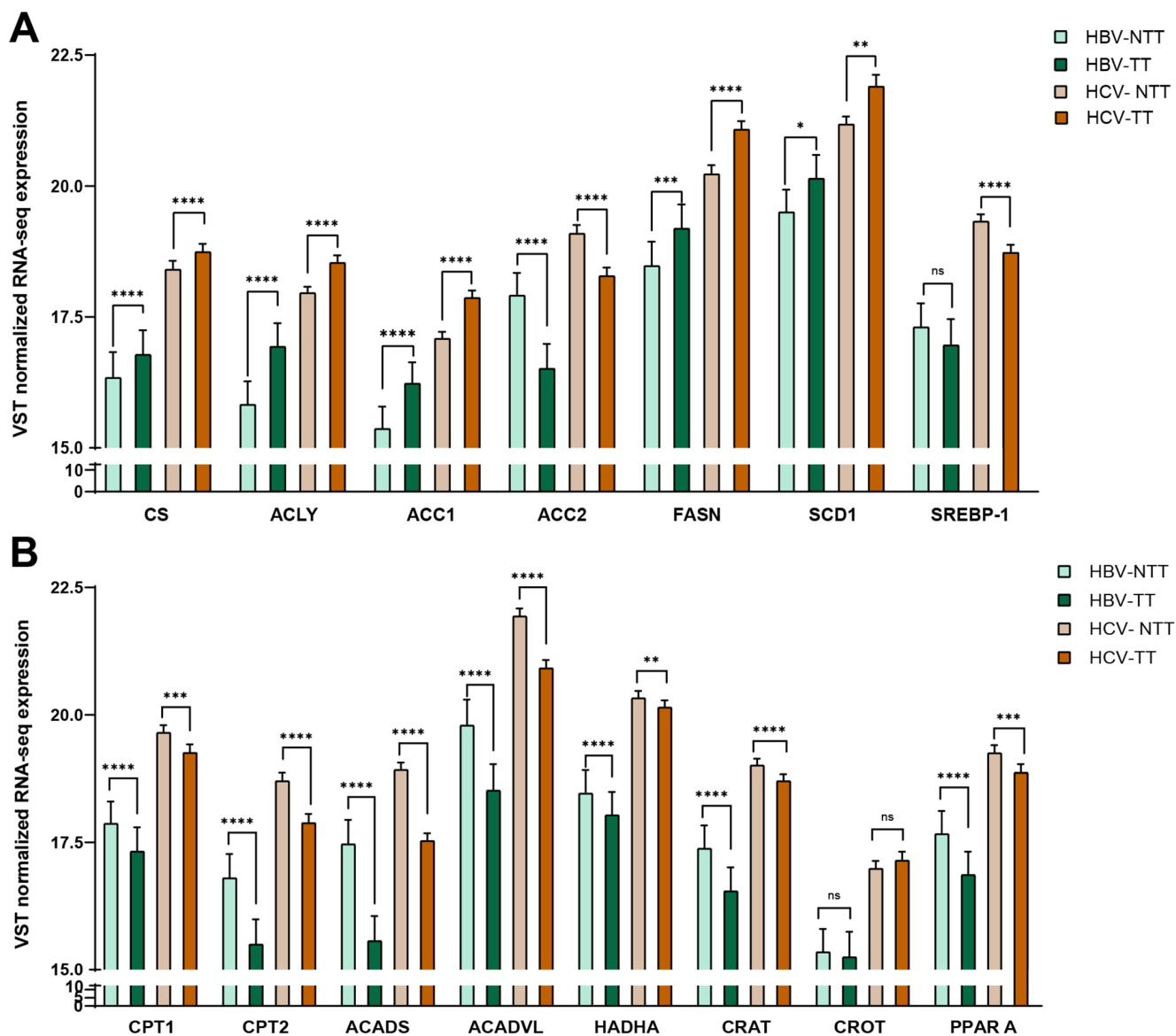
FIGURE 3 | Metabolic genes expression of VIRUS-HCC versus VIRUS-NTT by RNA-seq. Variance Stabilising Transformation (VST) normalised expression values of 7 genes (CS, ACLY, ACC1, ACC2, FASN, SCD1, SREBP-1) involved in the de Novo *lipogenesis* (DNL) pathway and 8 genes (CPT1, CPT2, ACADS, ACADVL, HADHA, CRAT, CROT, PPARA) involved the fatty acid oxidation (FAO) pathway in NTT versus TT tissue from HBV-related HCCs (A) and HCV-related HCCs (B). The data are expressed as the mean ± standard error of the mean (SEM). ns: no significant, *$p < 0.05$, **$p < 0.01$, ***$p < 0.001$, ****$p < 0.0001$ (Wilcoxon test).

In this report, an LC–MS analysis was employed to compare two groups of MASLD-HCC with their own adjacent tissues, revealing that AC were the main discriminant metabolites. AC are a class of lipids, the majority of which are derived from fatty acid oxidation, an essential biochemical process that generates energy from fat [18]. Prior research has documented an anomalous concentration of AC in HCC tissues, including elevated levels of LCAC and MCAC, along with diminished levels of SCAC. However, the majority of these reports pertains to HCC that has developed in the context of HBV and/or HCV infection [19–23]. Our study revealed that MASLD-HCC-F0F1-F2 is distinguished by an exclusive increase in LCAC whereas MASLD-HCC-F3F4 is characterised by an accumulation of both LCAC and MCAC, accompanied by a decrease in SCAC. The reduction in SCAC is consistent with the findings of our previous study, which employed ^{1}H-NMR spectroscopy and reported an accumulation of BCAA

in MASLD-HCC-F3F4 [12]. Moreover, it is noteworthy that MASLD-HCC-F3F4 displayed a distinctive metabolomic profile with multiple metabolites exhibiting downregulation. This suggests that in the presence of severe fibrosis, HCC may be more susceptible to metabolising substrates at a higher rate compared to their surrounding tissues. This metabolic reprogramming may indicate an increase in anabolism, potentially providing elevated supplies of essential building blocks for tumour cell growth.

The rise in AC in liver tissues, has been linked to a reduction in CPT2 protein synthesis in liver tissues of patients with VIRUS-HCC, indicating a down-regulation of FAO [19].

To the best of our knowledge, no report has addressed the AC profile in human MASLD-HCC tissues according to fibrosis status. Collectively, our metabolomic findings may suggest that:
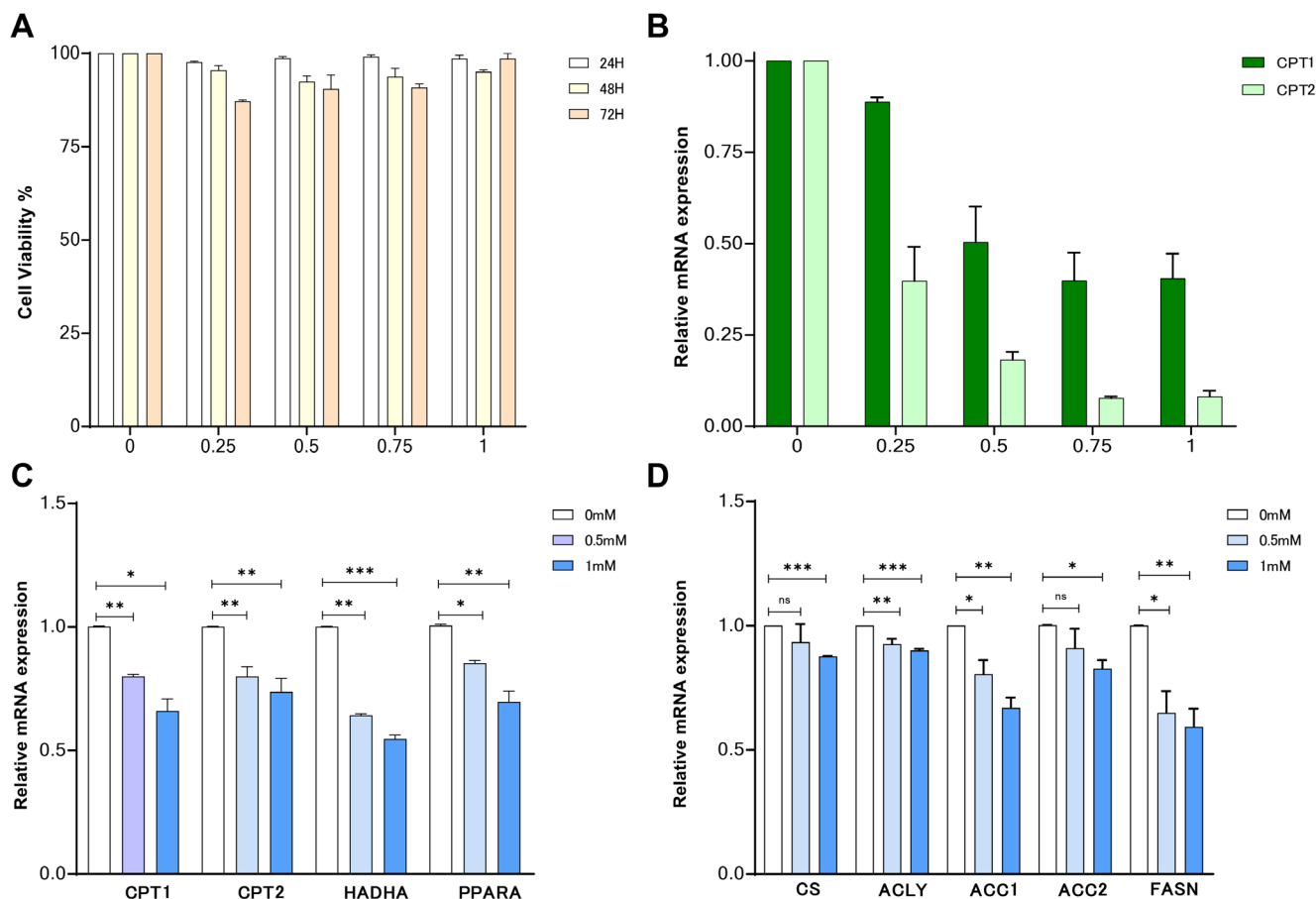
FIGURE 4 | Relative specific activity of CPT1 and CPT2 in HepG2 cell line. (A) The relative proliferation rates of the HepG2 cell line were evaluated following treatment with varying concentrations of amino-carnitine (0, 0.25, 0.75, or 1 mM) for 24, 48, or 72 h, in comparison to cells treated with the vehicle control. (B) The activity of CPT1 and CPT2 in HepG2 cells was measured in the presence or absence of amino-carnitine (24 h). The activities are expressed as the relative specific activity. The data are presented as means ± SEM ($n = 3$ experiments). (C, D) Expression profiles of HepG2 genes associated with the fatty acid oxidation (FAO) pathway and the de Novo lipogenesis (DNL) pathway. HepG2 cells were treated with amino-carnitine at concentrations of 0, 0.5, or 1 mM for a period of 24 h. The data are expressed as the mean ± standard error of the mean (SEM) with $n = 3$ experiments. NS: No statistically significant differences were observed, $*p < 0.05$, $**p < 0.01$, $***p < 0.001$ (Wilcoxon test).

(i) LCAC are sequestered in tumour tissues as compared with adjacent non-tumoral tissues, indicating a potential mechanism for tumour proliferation and or differentiation, and (ii) LCAC accumulation may be due to difficulties in transporting LCAC out of the liver, into the blood.

It is well established that tumour cells gain a survival and growth advantage by adapting their metabolism to respond to environmental stress. The most well-known aspect of metabolic transformation is the Warburg effect, whereby cancer cells up-regulate glycolysis under aerobic conditions [24]. However, the mechanisms mediating metabolic transformation that are not primarily associated with BCAA, FAO and DNL pathways remain undefined.

The two main enzymes involved in lipogenesis are ACC1 and FASN. ACLY is a strategic enzyme that links glycolytic and lipid metabolism in tumours [25]. It is well established that FASN is overexpressed in a number of human tumours and that its over-expression is significantly correlated with tumour aggressiveness and a poor prognosis [26, 27].

Furthermore, our findings confirm that the expression of enzymes involved in DNL, such as ACC1, FASN and SCD1, is over-expressed in both MASLD-HCC regardless of fibrosis level and in VIRUS-HCC [28–30].

The precise relationship between the severity of fibrosis in MASLD-HCC and FAO remains unclear. The present study demonstrates that the expression of genes encoding enzymes involved in the transport of AC, CPT1 and CPT2 is increased in MASLD-HCC in comparison to adjacent tumour tissues irrespective of the degree of fibrosis. Our findings are inconsistent with several studies on HCC that have reported a reduction in the expression of the genes encoding CPT1 and CPT2 genes in VIRUS-HCC [19, 28, 29]. Consequently, an identical gene panel was subjected to analysis in the VIRUS-HCC samples. Our results on VIRUS-HCC corroborate previously published findings indicating that the expression of genes encoding CPT1 and CPT2 was diminished in VIRUS-HCC relative to adjacent tissues [19, 31].

The existing literature relies mainly on VIRUS-HCC and posits that the downregulation of CPT2 in HCC results in the
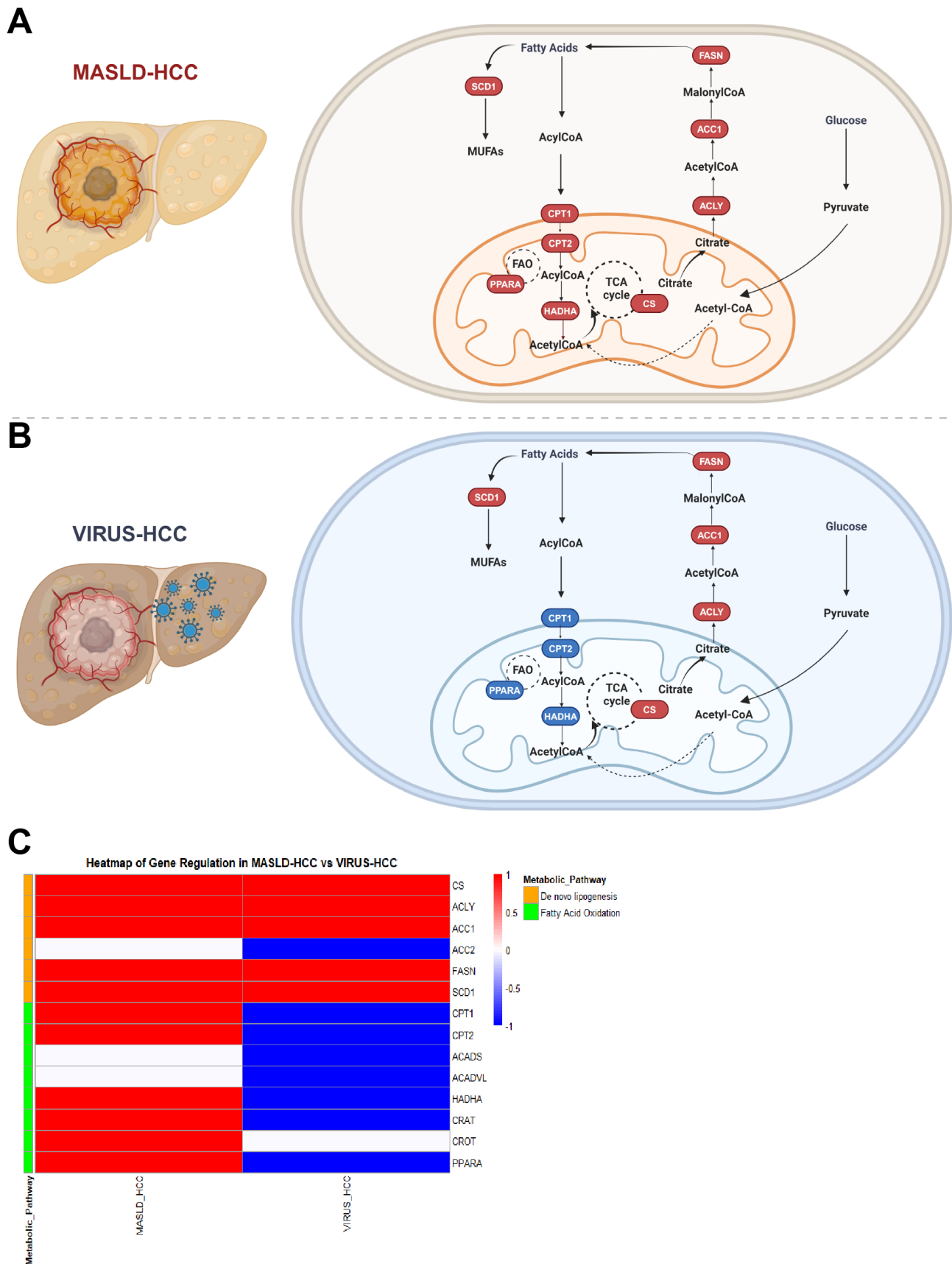
FIGURE 5 | Graphical representation showing the difference in de Novo Lipogenesis (DNL) and fatty acid oxidation (FAO) metabolic pathways. The expression levels of genes in (A) MASLD-HCC and (B) VIRUS-HCC are illustrated. Genes that are up- or down-regulated are indicated by red or blue, respectively. (C) A heatmap demonstrates the distinction in de Novo lipogenesis (DNL) and fatty acid oxidation (FAO) metabolic pathways between MASLD-HCC and VIRUS-HCC.

suppression of FAO, thereby enabling the cells to resist lipotoxicity and to better survive in a lipid-rich environment [28].

In parallel, we examine the expression of genes involved in DNL and FAO in HepG2 cells, treated with amino-carnitine, an inhibitor of the CPT system. Our findings indicate that amino-carnitine suppresses both FAO and DNL. This inhibition is more pronounced with CPT2 than with CPT1, corroborating prior findings [16, 17]. This reduction in enzyme activity coincides with a decline in protein levels. Consequently, amino-carnitine affects both enzyme activity and protein expression in HepG2 cells.

From our observations, we propose that MASLD-HCC may be more reliant on beta oxidation, which is consistent with the accumulation of AC as described in this report. The up-regulation of CROT and CRAT observed in the present study indicate that both mitochondrial and peroxisomal oxidation of AC occurred in MASLD-HCC, in contrast to the findings in VIRUS-HCC.

The expression of the six metabolic-related genes, involved in the FAO pathway, including CPT1, CPT2, HADHA, CRAT, CROT and PPARA is also elevated in MASLD-HCC whereas the expression of these same genes is either decreased or unaltered in VIRUS-HCC. These observations, based on a "omics" approach, suggest that different metabolic pathways are involved in the aetiology of HCC, as illustrated in Figure 5A,B,C.

The current study revealed that in MASLD-HCC, the up-regulation of the expression of metabolic-related genes involved in FAO is concomitant with the observed upregulation of DNL metabolic-related genes expression.

Our findings differ from those previously reported by other researchers, who demonstrated an alteration of genes implicated in β-oxidation in HCC. These genes were found to be down-regulated, including acyl-CoA dehydrogenase, HADHA and HADHB [31].

It has been reported that immunotherapy with ICIs was effective in VIRUS-HCC but provided little benefit in MASLD-HCC [32–34]. However, as it has been recently reported, the randomised controlled trials available to date have not been stratified according to aetiology, and data suggesting a possible impact of aetiology on the outcome of patients treated with immunotherapy come from subgroup analyses rather than pre-specified analyses [35].

One of the limitations of our study is that we utilised liver tissues from patients undergoing hepatectomy for HNF as a control group, and all the patients were female. It has been reported that the expression of specific genes, including PPARA is subjected to gender-dependent regulation [36]. However, despite the fact that the control tissue was derived from female subjects, no gender-related differences in the expression of genes involved in the FAO and DNL pathways of MASLD-HCC were observed in the present study (data not shown). Therefore, the results of this study are not influenced by gender. Moreover, two techniques were employed to investigate the expression of metabolic-related genes in MASLD-HCC and in VIRUS-HCC: qRT-PCR and RNA sequencing, respectively.

It is evident that further confirmation is required regarding the up-regulation of key activators of FAO in animal models. This can be achieved through the use of gene knockout (KO) models, which will facilitate a more detailed study of the function and the role of target genes.

5 | Conclusion

In general, the findings of this study indicated that, with regard to the degree of fibrosis, MASLD-HCCs exhibit distinctive profiles in their acyl-carnitine content. Moreover, the expression of genes related to metabolites indicates that the involvement of adaptive metabolic pathways differs depending on the aetiology of HCC. Therefore, the established dogma that posits the incompatibility of simultaneously activating FAO and DNL in cancerous cells does not apply to MASLD-HCC. These findings suggest that MASLD-HCC have adapted their metabolism to regulate an excessive lipid environment by accentuating the FAO process, irrespective of their score of fibrosis, degree of steatosis, or differentiation. In light of these findings, it seems reasonable to propose that the simultaneous activation of FAO and DNL may be considered as a hallmark of MASLD-HCC. These findings indicate that MASLD-HCC has a high energy demand, which is distinct from that observed in VIRUS-HCC. Additionally, the response to high energy demand involves a significant increase in the acetyl-CoA pool.

Consent

Informed consent was obtained from all subjects involved in the study.

Conflicts of Interest

The authors declare no conflicts of interest.

Data Availability Statement

The data that supports the findings of this study are available in the Supporting Information of this article.

References

1. F. Bray, J. Ferlay, I. Soerjomataram, R. L. Siegel, L. A. Torre, and A. Jemal, "Global Cancer Statistics 2018: GLOBOCAN Estimates of

Incidence and Mortality Worldwide for 36 Cancers in 185 Countries," *CA: A Cancer Journal for Clinicians* 68, no. 6 (2018): 394–424, https://doi.org/10.3322/caac.21492.

2. A. Desai, S. Sandhu, J. P. Lai, and D. S. Sandhu, "Hepatocellular Carcinoma in Non-Cirrhotic Liver: A Comprehensive Review," *World Journal of Hepatology* 11 (2019): 1–18, https://doi.org/10.4254/wjh.v11.i1.1.

3. Z. M. Younossi, A. B. Koenig, D. Abdelatif, Y. Fazel, L. Henry, and M. Wymer, "Global Epidemiology of Nonalcoholic Fatty Liver Disease-Meta-Analytic Assessment of Prevalence, Incidence, and Outcomes," *Hepatology* 64, no. 1 (2016): 73–84, https://doi.org/10.1002/hep.28431.

4. A. Koshy, "Evolving Global Etiology of Hepatocellular Carcinoma (HCC): Insights and Trends for 2024," *Journal of Clinical and Experimental Hepatology* 15, no. 1 (2025): 102406, https://doi.org/10.1016/j.jceh.2024.102406.

5. F. Piscaglia, G. Svegliati-Baroni, A. Barchetti, et al., "Clinical Patterns of Hepatocellular Carcinoma in Nonalcoholic Fatty Liver Disease: A Multicenter Prospective Study," *Hepatology* 63, no. 3 (2016): 827–838, https://doi.org/10.1002/hep.28368.

6. J. Ertle, A. Dechêne, J. P. Sowa, et al., "Non-alcoholic Fatty Liver Disease Progresses to Hepatocellular Carcinoma in the Absence of Apparent Cirrhosis," *International Journal of Cancer* 128, no. 10 (2011): 2436–2443, https://doi.org/10.1002/ijc.25797.

7. C. R. Wong, M. H. Nguyen, and J. K. Lim, "Hepatocellular Carcinoma in Patients With Non-alcoholic Fatty Liver Disease," *World Journal of Gastroenterology* 22 (2016): 8294–8303, https://doi.org/10.3748/wjg.v22.i37.8294.

8. X. Zha, Z. Gao, M. Li, X. Xia, Z. Mao, and S. Wang, "Insight Into the Regulatory Mechanism of m6A Modification: From MAFLD to Hepatocellular Carcinoma," *Biomedicine & Pharmacotherapy* 177 (2024): 116966, https://doi.org/10.1016/j.biopha.2024.116966.

9. F. Kanwal, J. R. Kramer, S. Mapakshi, et al., "Risk of Hepatocellular Cancer in Patients With Non-Alcoholic Fatty Liver Disease," *Gastroenterology* 155, no. 6 (2018): 1828–1837. e2, https://doi.org/10.1053/j.gastro.2018.08.024.

10. Y. Kawamura, Y. Arase, K. Ikeda, et al., "Large-Scale Long-Term Follow-Up Study of Japanese Patients With Non-Alcoholic Fatty Liver Disease for the Onset of Hepatocellular Carcinoma," *American Journal of Gastroenterology* 107, no. 2 (2012): 253–261, https://doi.org/10.1038/ajg.2011.327.

11. P. Golabi, J. M. Paik, K. Eberly, L. de Avila, S. A. Alqahtani, and Z. M. Younossi, "Causes of Death in Patients With Non-Alcoholic Fatty Liver Disease (NAFLD), Alcoholic Liver Disease and Chronic Viral Hepatitis B and C," *Annals of Hepatology* 27, no. 1 (2022): 100556, https://doi.org/10.1016/j.aohep.2021.100556.

12. B. Buchard, C. Teilhet, N. Abeywickrama Samarakoon, et al., "Two Metabolomics Phenotypes of Human Hepatocellular Carcinoma in Non-Alcoholic Fatty Liver Disease According to Fibrosis Severity," *Metabolites* 11, no. 1 (2021): 11010054, https://doi.org/10.3390/metabo11010054.

13. C. Teilhet, D. Morvan, J. Joubert-Zakeyh, et al., "Specificities of Human Hepatocellular Carcinoma Developed on Non-Alcoholic Fatty Liver Disease in Absence of Cirrhosis Revealed by Tissue Extracts ^{1}H-NMR Spectroscopy," *Metabolites* 7, no. 4 (2017): 7040049, https://doi.org/10.3390/metabo7040049.

14. J. Calderaro, G. Couchy, S. Imbeaud, et al., "Histological Subtypes of Hepatocellular Carcinoma Are Related to Gene Mutations and Molecular Tumour Classification," *Journal of Hepatology* 67, no. 4 (2017): 727–738, https://doi.org/10.1016/j.jhep.2017.05.014.

15. T. J. Hudson, W. Anderson, A. Aretz et al., "International Network of Cancer Genome Projects," *Nature* 464, no. 7291 (2010): 993–998, https://www.nature.com/articles/nature08987.

16. P. Li, Z. Xia, W. Kong, et al., "Exogenous L-Carnitine Ameliorates Burn-Induced Cellular and Mitochondrial Injury of Hepatocytes by Restoring CPT1 Activity," *Nutrition & Metabolism (London)* 18, no. 1 (2021): 65, https://doi.org/10.1186/s12986-021-00592-x.

17. M. Chegary, H. te Brinke, M. Doolaard, et al., "Characterization of l-Aminocarnitine, an Inhibitor of Fatty Acid Oxidation," *Molecular Genetics and Metabolism* 93, no. 4 (2008): 403–410, https://doi.org/10.1016/j.ymgme.2007.11.001.

18. S. H. Adams, C. L. Hoppel, K. H. Lok, L. Zhao, S. W. Wong, and P. E. Minkler, "Plasma Acylcarnitine Profiles Suggest Incomplete Long-Chain Fatty Acid β-Oxidation and Altered Tricarboxylic Acid Cycle Activity in Type 2 Diabetic African-American Women," *Journal of Nutrition* 139 (2009): 1073–1081, https://doi.org/10.3945/jn.108.103754.

19. Y. Lu, J. Chen, C. Huang, et al., "Comparison of Hepatic and Serum Lipid Signatures in Hepatocellular Carcinoma Patients Leads to the Discovery of Diagnostic and Prognostic Biomarkers," *Oncotarget* 9, no. 4 (2018): 5032–5043, https://doi.org/10.18632/oncotarget.23494.

20. S. Li, D. Gao, and J. Y. Function, "Detection and Alteration of Acylcarnitine Metabolism in Hepatocellular Carcinoma," *Metabolites* 9, no. 36 (2019): 36, https://doi.org/10.3390/metabo9020036.

21. K. Enooku, H. Nakagawa, N. Fujiwara, M. Kondo, T. Minami, and Y. Hoshida, "Altered Serum Acylcarnitine Profile Is Associated With the Status of Nonalcoholic Fatty Liver Disease (NAFLD) and NAFLD-Related Hepatocellular Carcinoma," *Scientific Reports* 9, no. 10663 (2019): 10663, https://doi.org/10.1038/s41598-019-47216-2.

22. L. Zhou, Q. Wang, P. Yin, W. Xing, Z. Wu, and S. Chen, "Serum Metabolomics Reveals the Deregulation of Fatty Acids Metabolism in Hepatocellular Carcinoma and Chronic Liver Diseases," *Analytical and Bioanalytical Chemistry* 403 (2012): 203–213, https://doi.org/10.1007/s00216-012-5782-4.

23. X. Cheng, X. Tan, W. Wang, Z. Zhang, R. Zhu, and M. Wu, "Long-Chain Acylcarnitines Induce Senescence of Invariant Natural Killer T Cells in Hepatocellular Carcinoma," *Cancer Research* 83 (2023): 582–594, https://doi.org/10.1158/0008-5472.CAN-22-2273.

24. O. Warburg, F. Wind, and E. Negelein, "The Metabolism of Tumors in the Body," *Journal of General Physiology* 8 (1927): 519–530, https://doi.org/10.1085/jgp.8.6.519.

25. E. D. Pope, E. O. Kimbrough, L. P. Vemireddy, P. K. Surapaneni, J. A. Copland, and K. Mody, "Aberrant Lipid Metabolism as a Therapeutic Target in Liver Cancer," *Expert Opinion on Therapeutic Targets* 23 (2019): 473–483, https://doi.org/10.1080/14728222.2019.1615883.

26. R. Shiragami, S. Murata, C. Kosugi, T. Tezuka, M. Yamazaki, and A. Hirano, "Enhanced Antitumor Activity of Cerulenin Combined With Oxaliplatin in Human Colon Cancer Cells," *International Journal of Oncology* 43 (2013): 431–438, https://doi.org/10.3892/ijo.2013.1978.

27. E. Sokolowska, M. Presler, E. Goyke, R. Milczarek, J. Swierczynski, and T. Sledzinski, "Orlistat Reduces Proliferation and Enhances Apoptosis in Human Pancreatic Cancer Cells (PANC-1)," *Anticancer Research* 37 (2017): 6321–6327, https://doi.org/10.21873/anticanres.12083.

28. N. Fujiwara, H. Nakagawa, K. Enooku, Y. Kudo, Y. Hayata, and T. Nakatsuka, "CPT2 Downregulation Adapts HCC to Lipid-Rich Environment and Promotes Carcinogenesis via Acylcarnitine Accumulation in Obesity," *Gut* 67 (2018): 1493–1504, https://doi.org/10.1136/gutjnl-2017-315193.

29. H. Suzuki, M. Kohjima, M. Tanaka, T. Goya, S. Itoh, and T. Yoshizumi, "Metabolic Alteration in Hepatocellular Carcinoma: Mechanism of Lipid Accumulation in Well-Differentiated Hepatocellular Carcinoma," *Canadian Journal of Gastroenterology and Hepatology* 2021 (2021): 8813410, https://doi.org/10.1155/2021/8813410.

30. J. Leslie, D. Geh, A. M. Elsharkawy, D. A. Mann, and M. Vacca, "Metabolic Dysfunction and Cancer in HCV: Shared Pathways and

Mutual Interactions," *Journal of Hepatology* 77 (2022): 219–236, https://doi.org/10.1016/j.jhep.2022.01.029.

31. E. Björnson, B. Mukhopadhyay, A. Asplund, N. Pristovsek, R. Cinar, and S. Romeo, "Stratification of Hepatocellular Carcinoma Patients Based on Acetate Utilization," *Cell Reports* 13 (2015): 2014–2026, https://doi.org/10.1016/j.celrep.2015.10.045.

32. D. Pfister, N. G. Núñez, R. Pinyol, et al., "NASH Limits Anti-Tumour Surveillance in Immunotherapy-Treated HCC," *Nature* 592, no. 7854 (2021): 450–456, https://doi.org/10.1038/s41586-021-03362-0.

33. J. Schwärzler, F. Grabherr, C. Grander, T. E. Adolph, and H. Tilg, "The Pathophysiology of MASLD: An Immunometabolic Perspective," *Expert Review of Clinical Immunology* 20, no. 4 (2024): 375–386, https://doi.org/10.1080/1744666X.2023.2294046.

34. G. K. Abou-Alfa, G. Lau, M. Kudo, et al., "Tremelimumab plus Durvalumab in Unresectable Hepatocellular Carcinoma," *NEJM Evidence* 1, no. 8 (2022): EVIDoa2100070, https://doi.org/10.1056/EVIDoa2100070.

35. N. Ganne-Carrié and P. Nahon, "Differences Between Hepatocellular Carcinoma Caused by Alcohol and Other Aetiologies," *Journal of Hepatology* 20 (2024), https://doi.org/10.1016/j.jhep.2024.12.030.

36. F. Djouadi, C. J. Weinheimer, J. E. Saffitz, et al., "A Gender-Related Defect in Lipid Metabolism and Glucose Homeostasis in Peroxisome Proliferator- Activated Receptor Alpha- Deficient Mice," *Journal of Clinical Investigation* 102, no. 6 (1998): 1083–1091, https://doi.org/10.1172/JCI3949.

Supporting Information

Additional supporting information can be found online in the Supporting Information section.